Desalination and Water Treatment
www.deswater.com
doi: 10.5004/dwt.2021.27895

244 (2021) 201–211
December

Synthesis and characterization of graphene oxide for removal of Cr(III) from tannery effluent

Sobur Ahmed[a], Fatema-Tuj-Zohra[a], Muhtasim M. Mahdi[a], Dewan Md. Mahmudunnabi[b], Tasrina R. Choudhury[c], Md. Zahangir Alam[b], Mohammad Nurnabi[b,*]

[a]*Institute of Leather Engineering and Technology, University of Dhaka, 44-50, Hazaribagh, Dhaka – 1209, Bangladesh, emails: soburahmed@du.ac.bd (S. Ahmed), fatema.ilet@du.ac.bd (F.-T. Zohra), miz40.mahdi@gmail.com (M.M. Mahdi)*
[b]*Applied Chemistry and Chemical Engineering, University of Dhaka, Dhaka – 1000, Bangladesh, ORCID: https://orcid.org/0000-0001-8245-6535; Tel. +8801552428255; Fax: +880-2-9667222; emails: nnabi@du.ac.bd (M. Nurnabi), dmmnabidu@gmail.com (D.M. Mahmudunnabi), zahangir@du.ac.bd (M.Z. Alam)*
[c]*Analytical Chemistry Laboratory, Atomic Energy Center, Bangladesh Atomic Energy Commission, Dhaka, Bangladesh, email: tasrina.rabia@gmail.com*

Received 26 June 2021; Accepted 12 October 2021

ABSTRACT

Chromium released with tannery effluent causes severe water pollution which is a great concern to the environment and public health. Removal of chromium from tannery effluent prior to discharging to the surface water is a crying need for protecting environment and human health. This article describes the preparation and characterization of graphene oxide (GO) and its adsorption potential for Cr(III) from hazardous chrome-tanning effluents. GO was characterized by X-ray diffraction analysis, field emission scanning electron microscopy, Fourier transform infrared spectroscopy, and Zeta potential measurement. Explanation of the adsorption mechanism, kinetics, and feasibility were also studied. The influence of different operational variables, for example, pH, adsorbent dosage, Cr(III) ion concentration, contact time, and temperature on adsorption of Cr(III) on GO were evaluated by batch experiments. Adsorption equilibrium of Cr(III) data matched with both Langmuir and Freundlich isotherms and the maximum adsorption capacity (q_m) was calculated from Langmuir isotherm and found as 366.3 mg/g. Cr(III) and other pollutants removal efficiency of GO was studied for the real effluent sample having Cr(III) concentration of 3,477.5 mg/L. At a GO dosage of 1.0 g/100 mL 51.88% Cr(III) was removed in just 20 min of treatment, while biochemical oxygen demand, chemical oxygen demand, and total dissolved solids removal was 57.93%, 55.41%, and 61.4%, respectively. The adsorption kinetics fitted well with a pseudo-second-order reaction model and thermodynamically it was spontaneous at lower temperature and exothermic in nature. Cr(III) loaded adsorbent was regenerated and reused for further adsorption.

Keywords: Adsorption capacity; Chromium sulfate; Zeta potential; Hummers' method; Regeneration

1. Introduction

Tanneries are the major users of trivalent chromium [$Cr(OH)SO_4$ salt] after the alloy and metal finishing industries. Around, 90% of the tanneries carry out chrome tanning process for leather tanning due to excellent hydrothermal stability and some other unique properties like the smoothness of grain, uniform elasticity, and resistance to atmospheric conditions, etc. [1,2]. During chrome-tanning, only 60% of the applied chrome salts are bound with

* Corresponding author.

the proteinous fibre (collagen) and the rest is disposed off with wastewaters containing 2,656–5,420 mg/L Cr(III), which is 1,000 times higher than its threshold value [3]. Unlike carcinogenic hexavalent chromium, Cr(III) is reported as less hazardous and noncorrosive. However, it also can cause several health hazards, for example, skin allergy, inflammation, nausea, DNA structure deformation, metabolic malfunction during prolonged exposure [4]. Therefore, the proper treatment of chrome-loaded tannery effluents is required before discharging into the environment.

Several techniques like precipitation, adsorption, ion exchange, membrane filtration, ozonization, photocatalytic degradation, bioremediation, chemical coagulation, and electrochemical oxidation, etc., have been reported for the treatment of Cr(III)-loaded tannery effluents [5]. Adsorption is preferable to others owing to its remarkable removal efficiency for wide-range of chemicals, low prices, and generating fewer secondary pollutants [6]. Activated carbon, biomass, zeolites, nanomagnetic materials, and metal organic framework-based materials are some popular adsorbents used for the remediation of hazardous pollutants including Cr(III) and Cr(VI) from wastewaters [7–15]. However, owing to the high price of available adsorbents, selective adsorbent for the removal of a particular pollutant, and not as much regeneration capability of some adsorbents, the researchers are nowadays looking for advanced and efficient adsorbent materials [16]. Scientific reports have shown that biomass-based materials produced from various agricultural and household activities are used as adsorbents for their low cost, easy availability, and significant adsorption capacity towards metals and metal ions [17]. However, none of these adsorbents has shown proficient metal adsorption capacity.

In this context, nanomaterials can become prominent adsorbents to eliminate Cr(III) from chrome tanning effluents. Nanomaterials possess a huge surface area and stabilize chemical configuration and surface charge, which have indicated their superiority for metal removal [18]. Recently, GO has been of interest as an adsorbent to remove contaminants from wastewaters. Compared to other adsorbent materials, GO possesses an extremely broad surface area (2,630 m^2/g), and various functional groups viz. hydroxyl, epoxy, and carboxylic groups facilitating adsorption capacity to contaminants [13,19]. Consequently, graphene oxide and its derivatives has become a centre of attraction in the research field of water purification [20]. The objectives of the current study was to explores the suitability of using graphene oxide as an adsorbent for Cr(III) from harmful effluent released after chrome-tanning. Additionally, the optimization of the sorption method, and evaluation of equilibrium, kinetics, and thermodynamic of the adsorption process were also enumerated.

2. Experimental

2.1. Materials

Graphite powder (99.5%), hydrogen peroxide (30%), sulfuric acid (98%), nitric acid (65%), potassium permanganate (97%), sodium nitrate, and hydrochloric acid (37%) were used for synthesis of graphene oxide. Chromium sulfate ($Cr_2(SO_4)_3 \cdot 6H_2O$ was used for preparing a standard solution of chromium(III). All chemicals were of analytical grade and used without further treatment.

2.2. Synthesis of graphene oxide

In this study, GO was prepared by modified Hummers' method [21]. Briefly, graphite powder (3.0 g) was added to a mixture (75 mL) of concentrated H_2SO_4 and concentrated HNO_3 (3:1) in a round bottom flask immersed in a water bath with vigorous stirring to form a homogeneous suspension, followed by addition of $KMnO_4$ (9.0 g) and $NaNO_3$ (1.5 g) slowly to the flask and left for overnight under stirring in a magnetic stirrer to yielded a thick paste. Then deionized water (120 mL) was added to it and stirred for 4 h in an oil bath at 35°C. A deep brown reaction mixture was produced, which was washed with deionized water (420 mL) followed by the addition of 30% H_2O_2 (20 mL) to produce a bright yellow mixture. Finally, 5% HCl (200 mL) was added to remove Mn^{2+} ions from the prepared graphene oxide and washed by adding deionized water followed by centrifugation at 5,000 rpm. Washing step was repeated several times until the pH of the solution was 7.0.

2.3. Wastewater collection

An adequate quantity of chrome-containing tannery wastewater (5 L) was collected in a sealed airtight plastic bottle following a standard method from the discharge point of Reliance Tannery Limited, Savar, Dhaka [22]. Collected wastewater sample was filtered to remove suspended particles and the filtrate was stored for metal analysis at 4°C to prevent hydrolysis.

2.4. Adsorbent characterization

Prepared GO sample was characterized by different analytical methods. Chemical nature and surface pattern of GO was identified with Fourier transform infrared spectroscopy (FTIR) and X-ray diffraction (XRD) analysis. Morphological characteristics of GO were evaluated by field emission scanning electron microscopy (FESEM). Ionic nature of GO surface was studied by measuring zeta potential charge (ZPC) with zeta potential analyzer (Nano-ZS ZEN 3600).

2.5. Batch experiments

Batch experiments were carried out to investigate the role of different parameters, such as pH, adsorbent dose, contact time, and initial concentration of chromium ions for optimizing adsorption. The residual concentration of metal ions in the treated wastewater sample was determined with an atomic absorption spectrophotometer (AAS). Rate of metal removal and adsorption capacity of the adsorbent were calculated as follows:

Adsorption capacity at time *t*,

$$q_t = \frac{\left(C_0 - C_t\right) \times V}{w} \tag{1}$$

$$\% \text{ of removal} = \frac{\left(C_0 - C_e\right)}{C_e} \times 100 \tag{2}$$

Adsorption capacity at equilibrium,

$$q_e = \frac{(C_0 - C_e) \times V}{w} \quad (3)$$

where C_0 = initial Cr(III) concentration of solution (mg/L), C_t = concentration of Cr(III) in solution at time t (mg/L), C_e = concentration of Cr(III) in solution at equilibrium (mg/L), V = volume of the solution (L), and W = mass of the adsorbent (g).

3. Results and discussion

3.1. Synthesis and characterization of prepared GO

In the present study, grapheme oxide was synthesized from graphite which is a cheap and available material following modified Hummer's method [21]. The synthetic route is represented Fig. 1. When the GO suspension is acidic, it was easily precipitated and at ear neutral pH dispersibility of GO was too high to separate it. Thus, purification of GO prepared by this process is a lengthy and tedious step, however, it can be facilitated significantly by using centrifuge.

3.1.1. XRD analysis

The XRD pattern of synthesized GO is shown in Fig. 2. A broad peak observed at 2θ = 10.399° corresponding to an interlayer spacing of 8.5 Å, which is consistent with the literature value of 2θ = 11.4° and *d*-spacing = 7.8 Å [23].

3.1.2. Microscopic analysis

The morphology of the GO samples was assessed by FESEM. Fig. 3 shows the scanning electron microscopy (SEM) images of GO at 20,000× and 10,000× magnification. The working distance is about 6.6 mm at high vacuum mode with 5.0 kV. The image has shown fluffy, randomly aggregated and wrinkled sheets with a wide-ranged orientation of hierarchical pores that play the major roles in adsorbing metal ions [24]. This fluffiness and wrinkles in the GO are ensued due to oxidation and layer separation. Tan et al. [25] observed the same result in the SEM structure of their synthesized graphene oxide membrane which was used for the adsorption of some selected heavy metal ions from an aqueous solution.

The FESEM of GO after adsorption of Cr(III) showed a uniform surface (Fig. 3b). It is assumed that this is due to the binding of Cr(III) ions on the activated sites of the pores present on GO surface. Similar results were reported by White et al. [26] during copper (Cu^{2+}) adsorption onto graphene oxide (GO) and functionalized GO nanoparticles.

3.1.3. FTIR analysis

FT-IR spectra of graphene oxide shown in Fig. 4 exhibits some distinguished absorption peaks at different wave numbers in the infrared region corresponding to the existence of various functional groups. A strong and broad O–H stretching vibration band at 3,414 cm^{-1} was because of extensive oxidation occurring at GO surface. The significant peaks were due to C–H stretching vibration at 2,989 cm^{-1}, C=O stretching vibration band of the carboxylic group at 1,732 cm^{-1}, aromatic C=C stretching band at 1,519 cm^{-1}, symmetric C–O stretching in the C–O–C group at 1,209 cm^{-1} and the C–O (epoxy) band at 964 cm^{-1}. The FT-IR spectra of graphene oxide showed a good agreement with the previous studies [27,28].

3.2. Effect of operational parameters on Cr(III) adsorption capacity of GO

3.2.1. Effect of pH

To study the effect of pH on the adsorption of Cr(III) on GO, 20 mL trivalent chromium salt solution of known concentration (245.5 ppm) was taken in each of four conical flasks and pH was adjusted to 2.0, 3.0, 4.0, and 5.0 and loaded with GO (0.039 g). The mixture was agitated in an

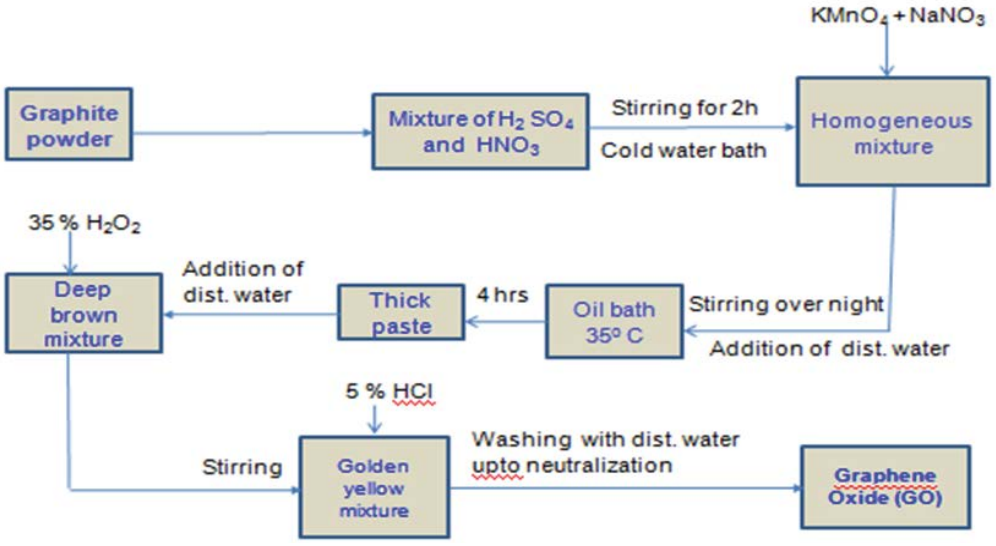

Fig. 1. Flow chart for synthesis of GO.

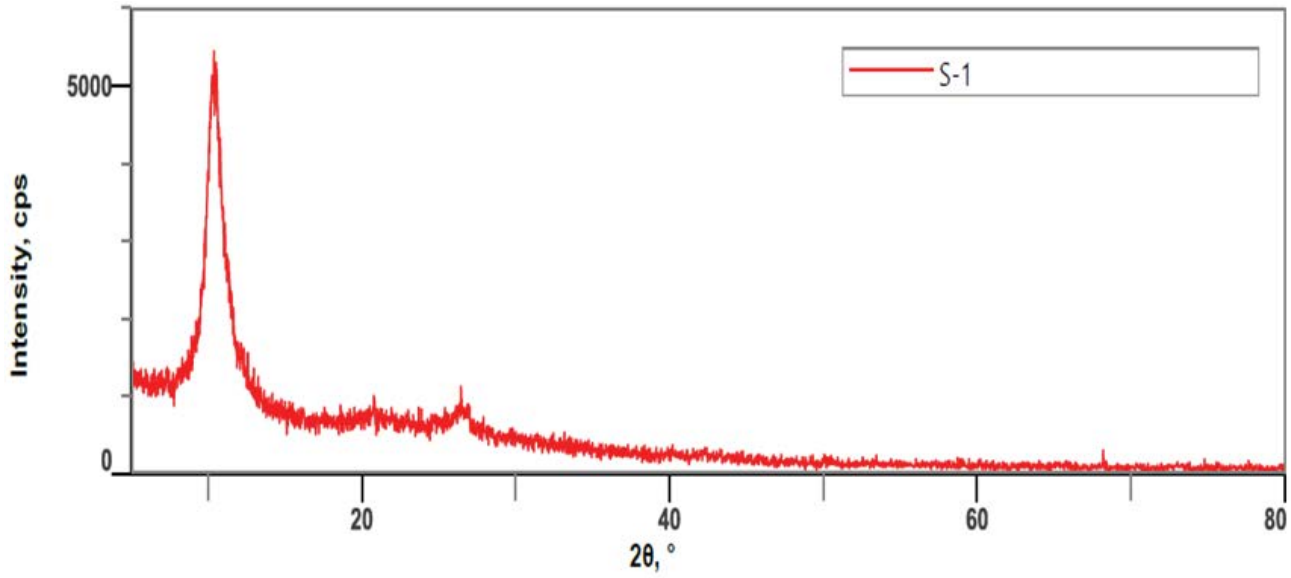

Fig. 2. XRD of GO.

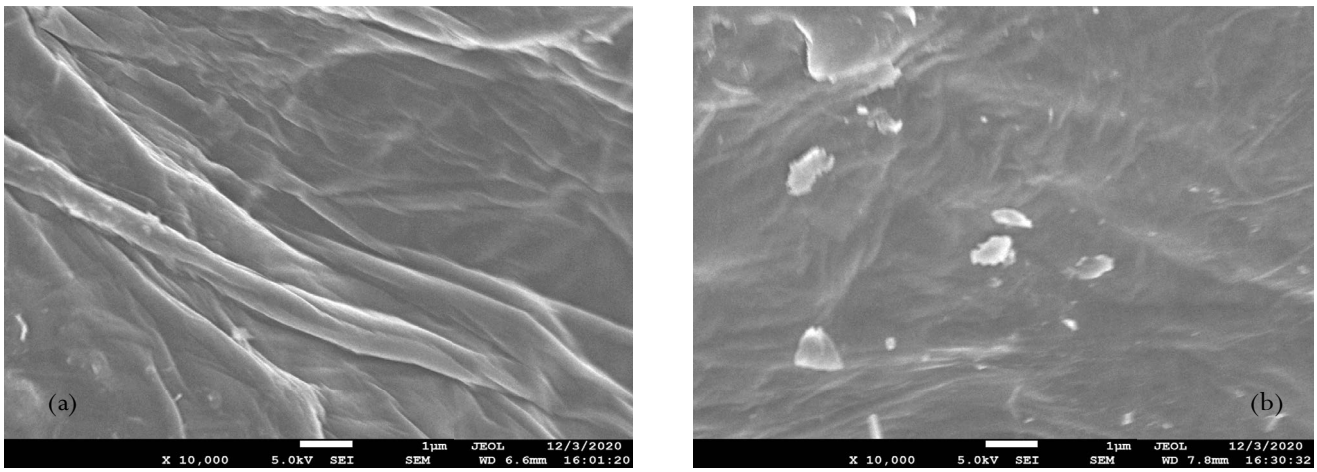

Fig. 3. FESEM images of (a) fresh GO and (b) Cr(III) loaded GO.

orbital shaker at 150 rpm for 2 h at ambient temperature, adsorption capacity was calculated and the result was as presented in Fig. 5b. The results revealed that the adsorption of Cr(III) is minimum at pH and increased gradually with increasing pH and reached the maximum at pH 4.0. Zeta potential of GO suspension at different pH revealed that the surface charge of GO became zero at a pH (pH_{ZPC}) less than but close to pH 4.0 as shown in Fig. 5a. Thus, at pH lower than pH_{ZPC} carboxyl groups at active sites were protonated and the surface became positively charged, while at pH 4.0, which is higher than pH_{ZPC}, the carboxyl groups of GO is deprotonated and the surface becomes negatively charged. On the other hand at pH also significantly influence the existence of Cr(III) species in aqueous solutions. At pH < 3.0 it is present as Cr^{3+}, while at pH around 4.0, it exists as a mixture of Cr^{3+} and $Cr(OH)^{2+}$ [29]. From electrostatic point of view, at lower pH than pH_{ZPC} repulsion between the positively charged GO surface and cationic Cr-species occurred, while at pH higher than pH_{ZPC} strong attraction forces played vital role in adsorption process [29,30]. However, chromium is precipitated from an aqueous solution as $Cr(OH)_3$ at higher pH higher than 6.0 and the study was not conducted at a higher pH [31].

3.2.2. Effect of adsorbent dosage

To optimize the dosage of GO a series of conical flasks containing 10 mL standard chromium salt solution (245.5 ppm) in each of them were treated with different dosages of GO (0.25, 0.5, 1.0, 1.5, and 2.0 g/L) at the optimum pH (4.0) and agitated in an orbital shake. The experimental results revealed that the removal efficiency was increased with an increase in adsorbent dosages and the optimum dosage was 0.6 g/L (Fig. 6). At higher dosage the number of active sites increased and the number of metal ions binding to the active sites also increased and demonstrated higher

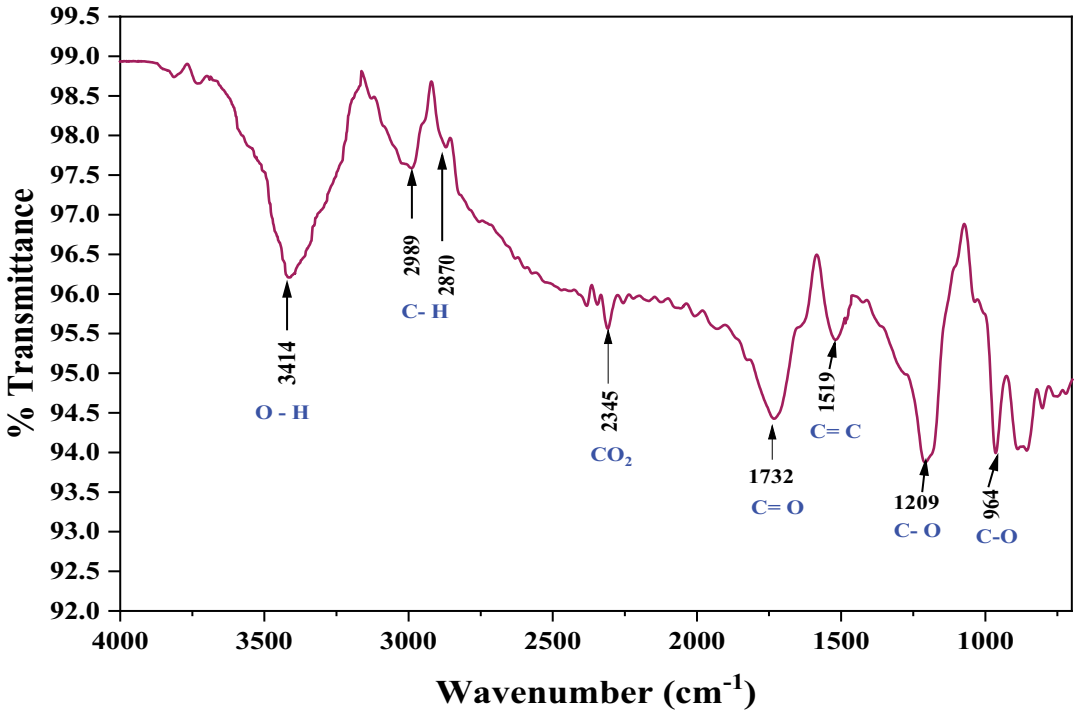

Fig. 4. FT-IR spectrum of prepared GO.

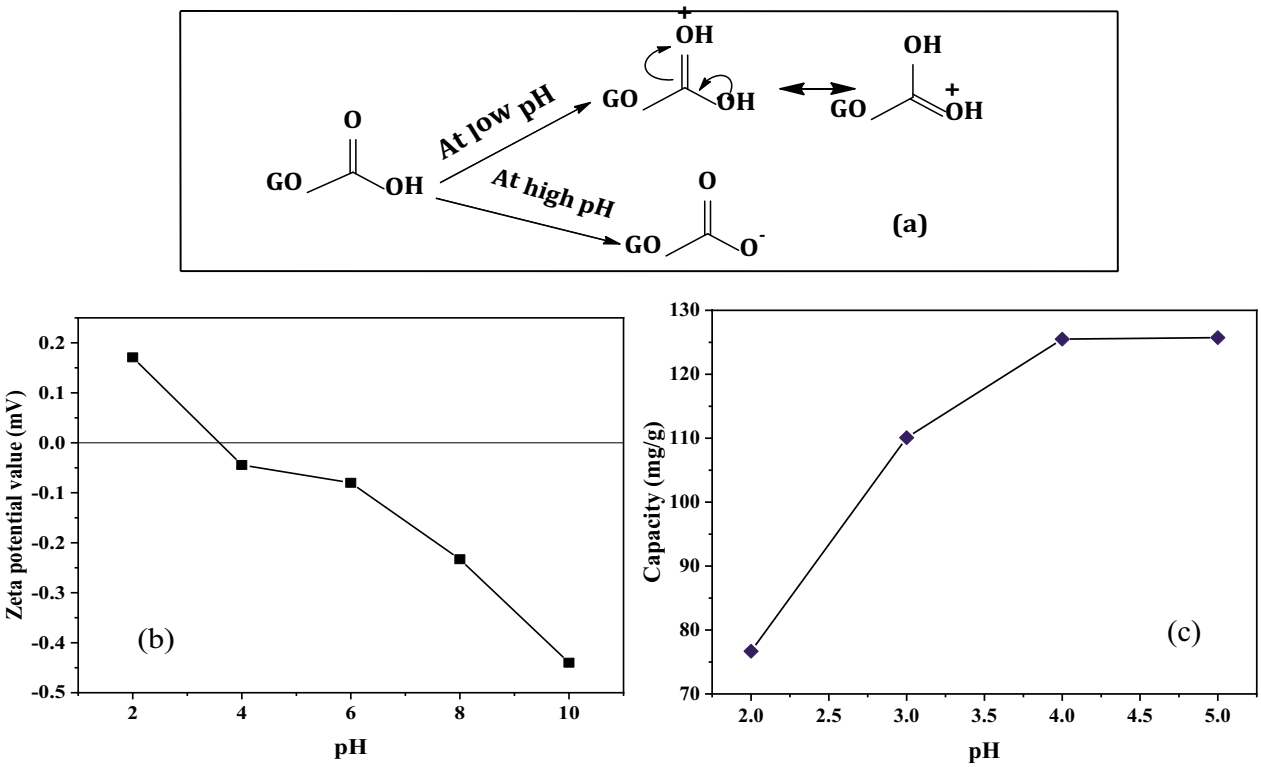

Fig. 5. Effect of pH on (a) ionic state of GO, (b) zeta potential value of GO, and (c) Cr(III) adsorption onto GO.

percentage of removal [32]. Qiu et al. [33] reported similar results in case of removing Cr(III) with sludge-derived biochar with supported nano-zero-valent iron. However, the sorption capacity reduced with increasing dosages, which may be attributed to the fact that many active sites were left vacant at a higher dosage [34].

3.2.3. Effect of contact time and metal concentration

Batch experiments were conducted to determine the effects of contact time and initial Cr(III) concentration on adsorption capacity on GO (Fig. 7). The experiments were carried out by treating 10 mL chromium(III) solution of different concentrations (104.22, 125.4, 174, and 198.57 ppm) with a fixed adsorbent dosage (0.6 g/L) at optimum pH (4.0) for a predetermined time interval (0–120 min). As evident from Fig. 7, adsorption process is quick and reached the equilibrium in just 20 min. Then no significant changes were observed in the adsorption process with increasing contact time. Abshirini et al. [32] proposed that the vacant active sites present on the adsorbent surface start to get occupied by the adsorbate with increasing contact time resulting in an increase in sorption capacity, and has no significant effect once the process reaches the equilibrium.

The initial metal concentration in the solution is one of the most significant driving forces in the adsorption process. It provides a brief description of the relationship of mass transfer and mass balance between the solutes in a liquid phase (adsorbate) and solid phase (adsorbent) [35]. Fig. 7 illustrated that the adsorption capacity was increased with an increase in initial chromium concentration. At a higher concentration of metal ions, the number of activated sites is nearly equal to that causing higher metal uptake [36].

3.3. Studies on equilibrium isotherms

The sorption mechanism was studied through establishing a relationship between adsorbate and adsorbent at equilibrium condition [37]. It also measures the maximum adsorption capacity of an adsorbent for a particular adsorbate [38,39]. In this study, the sorption data were interpreted employing two most widely used isotherm models, such as Langmuir [Eqs. (4) and (5)] and Freundlich [Eq. (6)] isotherms [40]:

$$\frac{C_e}{q_e} = \frac{1}{q_m b} + \frac{1}{q_m} C_e \tag{4}$$

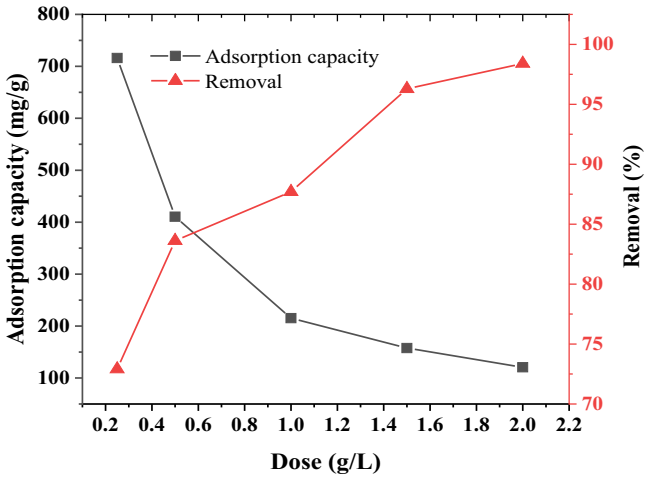

Fig. 6. Effect of GO dosage on Cr(III) adsorption.

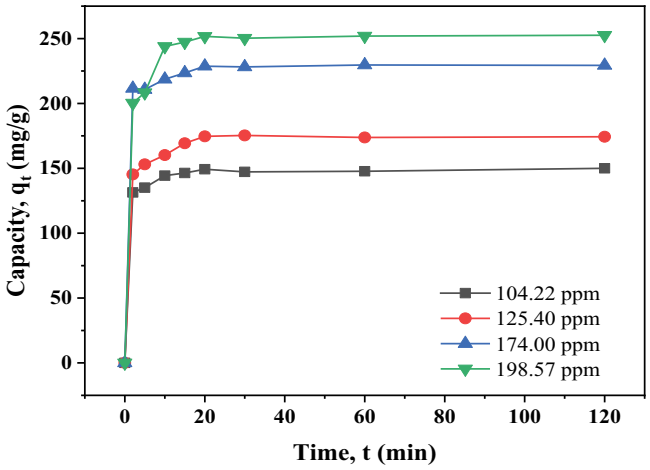

Fig. 7. Effect of initial Cr(III) concentration and contact time on adsorption capacity onto GO.

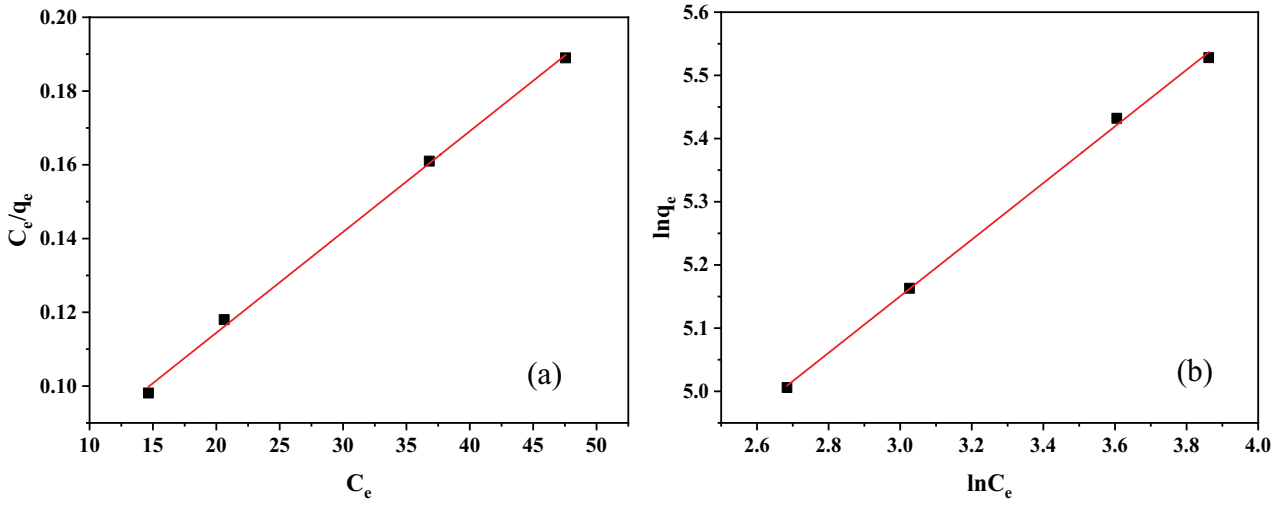

Fig. 8. Isotherm models for Cr(III) adsorption on GO (a) Langmuir and (b) Freundlich isotherms.

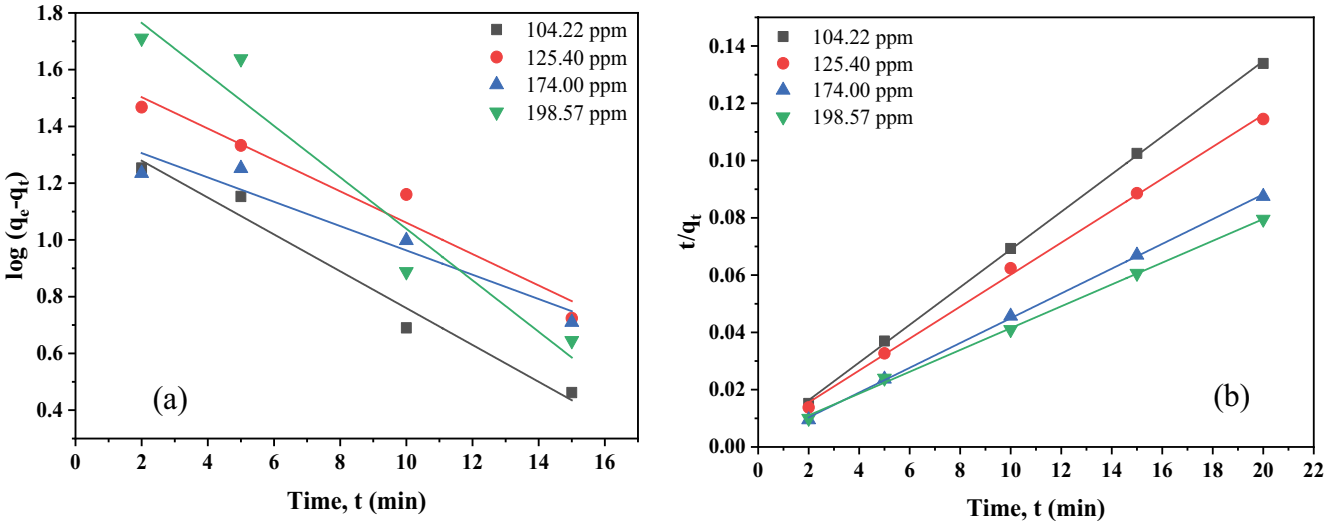

Fig. 9. Kinetic models (a) pseudo-first-order and and (b) pseudo-second-order reaction for Cr(III) adsorption on GO.

$$R_L = \frac{1}{1 + C_m b} \tag{5}$$

$$\ln q_e = \ln K_F + \frac{1}{n} \ln C_e \tag{6}$$

where q_e = amount of adsorbed metal in per unit mass of adsorbent (mg/g), C_e = equilibrium metal concentration (mg/L), q_m = maximum adsorption capacity (mg/g), b = Langmuir constant (L/mg), R_L = separation factor, and C_m = maximum metal ion concentration.

The results are presented in Table 1 and it was clear from figure 8 that the adsorption of Cr(III) onto GO surfaces followed both the Langmuir and Freundlich isotherm models (R^2 = 0.998) indicating that the process proceeded with the formation of both monolayer and multilayer of metal ions on GO surface. However, value of R_L was 0.098 and this value $0 < R_L < 1$ strongly supports the favourable monolayer adsorption process [41]. The maximum adsorption capacity was obtained from the Langmuir model and was 366.3 mg/g. These results are in good agreement with the report published by Mondal and Chakraborty [42]. Value of adsorption intensities (n) was calculated from Freundlich isotherm and found to be 2.232. The value of $0 < n < 10$ stands for favorable adsorption, thus adsorption of Cr(III) on GO is favored [41].

Table 1
Isotherm constants for Cr(III) adsorption onto GO

Langmuir constants	Values	Freundlich constants	Values
q_m (mg/g)	366.3	K_F	45.02
b (L/mg)	0.046	n	2.232
R^2	0.998	R^2	0.998
R_L	0.098		

3.4. Kinematic studies

Adsorption kinetics depicts the effect of metal ion concentration and the available active sites on the adsorption rate. Two most popular kinetic models such as pseudo-first-order [Eq. (7)] and pseudo-second-order [Eq. (8)] kinetic models were employed to understand the sorption of Cr(III) on GO. The following equations were applied to measure the kinetic parameters:

$$\log\left(q_e - q_t\right) = \log q_e - \left(\frac{k_1}{2.303}\right) t \tag{7}$$

$$\frac{t}{q_t} = \left(\frac{1}{k_2 q_e^2}\right) + \left(\frac{1}{q_e}\right) t \tag{8}$$

where q_e and q_t denote amount of adsorbed ion adsorbed per unit mass of adsorbent (mg/g) at equilibrium and at time t, respectively, k_1 and k_2 represent adsorption constant for pseudo-first-order reaction and pseudo-second-order kinetics.

From figure 9 it is evident that the findings of the experimental works fitted best with the pseudo-second-order kinetic model with a regression coefficient value (R^2) of 0.999 (Table 2). A similar result was also observed in some previous studies based on graphene oxide and its derivatives for removing Cr(III) ions from aqueous solutions [43–46]. This information also points towards the chemisorption nature of the adsorption process. Therefore, a strong attraction force between the anionic functional groups (carboxylates) of GO and metal ions were present [47].

3.5. Thermodynamic study

Thermodynamic study of an adsorption process ascertains its randomness and feasibility based on temperature [16]. The removal of Cr(III) by GO was evaluated at different temperatures (293–338 K) and the thermodynamic parameters were determined (Table 3). Gibbs free energy change (ΔG) was calculated using van't Hoff isotherm [Eq. (9)] [48], where K_d was the ratio of q_e to C_e:

Table 2
Summary of adsorption kinetics

Kinetics model	Parameters	104.22 ppm	125.40 ppm	174.00 ppm	198.57 ppm
Pseudo-first-order	q_e^* (mg/g)	25.64	41.11	24.66	88.31
	k_1	0.149	0.127	0.0986	0.2089
	R^2	0.974	0.953	0.931	0.941
	q_e^{**} (mg/g)	149.28	174.63	228.63	251.7
Pseudo-second-order	q_e^* (mg/g)	152.21	179.21	230.95	262.47
	k_2	0.0135	0.0071	0.011	0.0042
	R^2	0.999	0.998	0.999	0.998
	q_e^{**} (mg/g)	149.28	174.63	228.67	251.70

*Theoretical, **Experimental

Table 3
Thermodynamic parameters of Cr(III) adsorption on GO

T (K)	ΔG (kJ/mole)	ΔH (kJ/mole)	ΔS (kJ/mole)
293	–7.197	–37.147	–0.0981
308	–6.54		
323	–5.433		
338	–4.314		

$$\Delta G = -RT\ln K_d \tag{9}$$

The linearized van't Hoff isotherm [Eq. (10)] and its plot is shown in the Fig. 10 and change of enthalpy (ΔH) and entropy (ΔS) were determined by measuring the slope and intercept of the straight line obtained from the plot.

$$\ln K_d = \frac{-\Delta H}{RT} + \frac{\Delta S}{R} \tag{10}$$

Considering the change of free energy and enthalpy, it was evident that the sorption process was spontaneous and exothermic.

3.6. Regeneration of GO

To study the potential re-use of Cr(III) loaded GO it was regenerated using 2% HCl and reused for Cr(III) adsorption at optimum pH, adsorbent dosage and time. The results of regeneration and reuse studies showed that adsorption capacity slowly decreased from 150.85 to 142.87, 118.23 and 68.92 mg/g after recycle-1, recycle-2 and recycle-3, respectively (Table 4). Thus, regenerated GO can be reused for the removal of Cr(III) from the aqueous solution.

3.7. Evaluation of physicochemical parameters

Several physicochemical parameters of wastewater sample were measured before and after adsorption and the results are presented in Table 5, that showed significant improvements in the physicochemical parameters after the treatment of effluent samples with GO. It proved that GO

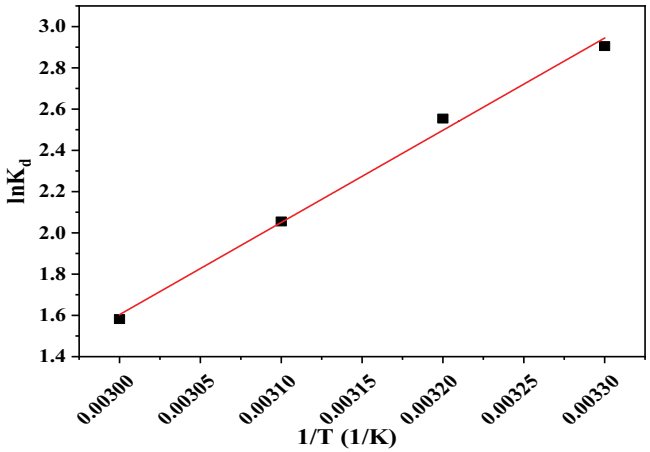

Fig. 10. Plot for van't Hoff isotherm.

Table 4
Adsorption capacity of regenerated graphene oxide

Regenerated GO	Capacity (mg/g)
Fresh GO	150.85
Recycle-1	142.87
Recycle-2	118.23
Recycle-3	68.92

can simultaneously remove Cr(III) and other organic pollutants from real tannery wastewater.

3.8. Plausible adsorption mechanism of Cr(III) on GO

The adsorption mechanism may involve hydrogen bonding, electrostatic or π–π interactions, vander Waals forces, dipole–dipole induction, ion-exchange etc. In the present study the adsorption of Cr(III) on GO surface was mainly electrostatic interaction as the maximum adsorption was obtained at pH 4.0, which is greater than pH_{ZPC} of GO and thus graphene oxide possesses a negative surface and at this pH Cr(III) exists as a mixture of Cr^{3+} and $Cr(OH)^{2+}$ [29]. Thus, a strong electrostatic interaction played the vital role for retention of Cr-ions on GO surface. It was

Table 5
Changes in physicochemical parameters of the tanning effluent after adsorption[a]

Parameters	Before adsorption	After adsorption	% of removal	ECR, 1997 [49]
Cr(III) concentration (ppm)	3,477.5	1,673.25	51.88	2.0
Adsorption capacity (mg/g)	–	180.43	–	–
pH	4.1	5.3	–	6–9
TDS (ppm)	5,135	1,982	61.4	2,100
EC (μS/cm)	10,165	3,967	60.97	–
NaCl (%)	17.6	6.8	61.36	–
BOD_5 (ppm)	4,643	1,953	57.93	100
COD (ppm)	12,164	5,424	55.41	–

Adsorbent dosage was 1.0 g/100 mL effluent.

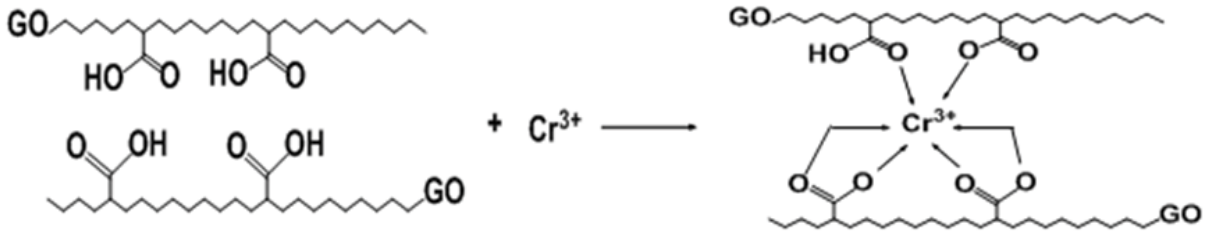

Fig. 11. Adsorption mechanism of Cr(III) on GO.

Table 6
Comparison of Cr(III) adsorption on GO and other adsorbents

Adsorbent name	pH	Adsorbent dose	Initial Cr(III) concentration	Contact time	% Removal	q_{max} (mg/g)	Reference
Fish scale	5	0.8 g	150 mg/L	90 min	99.7518	18.3486	[50]
GO/alginate hydrogel membrane	6	–	40 mg/L	60 min		118.6	[51]
Activated carbon	4		200 mg/L	3–5 months			[52]
Graphene oxide	4	0.6 g/L	174 mg/L	20 min	98.77	366.3	This work

presumed that Cr(III) formed hexacoordinate complexes with caboxylates of the GO surface (Fig. 11).

3.9. Effectiveness of GO as adsorbent

Recently, GO and its derivatives have gained much attention from researchers as prominent adsorbents for removing pollutants from water bodies. Therefore, the compatibility of GO on Cr(III) removal was compared with other adsorbents in Table 6 that showed remarkable metal uptake compared to the most other adsorbents reported earlier.

4. Conclusion

Graphene oxide was synthesized from graphite powder by Hummer's method and characterized by XRD, FE-SEM, FT-IR, etc. FT-IR analysis ascertained that the surface of GO contained carboxylic acid functional group. Zeta potential measurement at different pH revealed that GO surface was of zero charge at a pH close to 4.0 (pH_{ZPC}). The synthesized GO was then applied for removal of Cr(III) by adsorption process. Optimum pH and dosage were 4.0 and 0.6 g/L respectively. The adsorption process was quick and reached equilibrium in just 20 min. Adsorption of Cr(III) on GO followed both Langmuir and Freundlich isotherm models and the maximum adsorption capacity was 366 mg/g. Kinetic studies showed that it followed a pseudo-second-order reaction mechanism. Change in Gibb's free energy, enthalpy, and entropy were determined using van't Hoff isotherm equation and found that the process was spontaneous [negative (ΔG)] and exothermic in nature [negative (ΔH)]. Used GO was regenerated and reused successfully. The synthesized material (GO) was applied to treat real tannery effluent and found effective for wastewater containing extremely high Cr(III), BOD_5 and COD contents. However, further studies are necessary to develop industrially usable adsorbent based on GO.

Acknowledgments

The authors would like to thank the authorities of Department of Applied Chemistry and Chemical Engineering

and Institute of Leather Engineering and Technology (ILET), University of Dhaka and Atomic Energy Center, Bangladesh Atomic Energy Commission, Dhaka, Bangladesh for providing the lab facilities and testing supports.

References

[1] S. Ahmed, Fatema-Tuj-Zohra, M.S.H. Khan, M.A. Hashem, Chromium from tannery waste in poultry feed: a potential cradle to transport human food chain, Cogent. Environ. Sci., 3 (2017) 1312767, doi: 10.1080/23311843.2017.1312767.
[2] C.K. Ozkan, H. Ozgunay, H. Akat, Possible use of corn starch as tanning agent in leather industry: controlled (gradual) degradation by H_2O_2, Int. J. Biol. Macromol., 122 (2019) 610–618.
[3] M.A. Hashem, M. Hasan, M.A. Momen, S. Payel, M.S. Nur-A-Tomal, Water hyacinth biochar for trivalent chromium adsorption from tannery wastewater, Environ. Sustainability Indic., 5 (2020) 100022, doi: 10.1016/j.indic.2020.100022.
[4] R.T. Achmad, E.I. Auerkari, Effects of chromium on human body, Ann. Res. Rev. Biol., 17 (2017) 1–8.
[5] M. Nur-E-Alam, M.A.S. Mia, F. Ahmad, M.M. Rahman, An overview of chromium removal techniques from tannery effluent, Appl. Water Sci., 10 (2020) 1–22.
[6] Y. Priastomo, H.R. Setiawan, Y.S. Kurniawan, K. Ohto, Simultaneous removal of lead(II), chromium(III), and copper(II) heavy metal ions through an adsorption process using C-phenylcalix [4] pyrogallolarene material, J. Environ. Chem. Eng., 8 (2020) 103971, doi: 10.1016/j.jece.2020.103971.
[7] M. Fazal-ur-Rehman, Methodological trends in preparation of activated carbon from local sources and their impacts on production: a review, Chem. Int., 4 (2018) 109–119.
[8] A. Zubair, H.N. Bhatti, M.A. Hanif, F. Shafqat, Kinetic and equilibrium modeling for Cr(III) and Cr(VI) removal from aqueous solutions by *Citrus reticulata* waste biomass, Water Air Soil Pollut., 191 (2008) 305–318.
[9] H.N. Bhatti, A.W. Nasir, M.A. Hanif, Efficacy of *Daucus carota* L. waste biomass for the removal of chromium from aqueous solutions, Desalination, 253 (2010) 78–87.
[10] A.R. Iftikhar, H.N. Bhatti, M.A. Hanif, R. Nadeem, Kinetic and thermodynamic aspects of Cu(II) and Cr(III) removal from aqueous solutions using rose waste biomass, J. Hazard. Mater., 161 (2009) 941–947.
[11] H.N. Bhatti, M. Yasir, Removal and recovery of Al(III) and Cr(VI) from aqueous solution by waste black tea, Environ. Eng. Manage. J., 5 (2016) 809–816.
[12] F. Liu, S. Hua, C. Wang, M. Qiu, L. Jin, B. Hu, Adsorption and reduction of Cr(VI) from aqueous solution using cost-effective caffeic acid functionalized corn starch, Chemosphere, 279 (2021) 130539, doi: 10.1016/j.chemosphere.2021.130539.
[13] R. Wijaya, G. Andersan, S.P. Santoso, W. Irawaty, Green reduction of graphene oxide using kaffir lime peel extract (*Citrus hystrix*) and its application as adsorbent for methylene blue, Sci. Rep., 10 (2020) 1–9.
[14] J. Li, X. Wang, G. Zhao, C. Chen, Z. Chai, A. Alsaedi, T. Hayat, X. Wang, Metal-organic framework-based materials: superior adsorbents for the capture of toxic and radioactive metal ions, Chem. Soc. Rev., 47 (2018) 2322–2356.
[15] X. Liu, H. Pang, X. Liu, Q. Li, N. Zhang, L. Mao, M. Qiu, B. Hu, H. Yang, X. Wang, Orderly porous covalent organic frameworks-based materials: superior adsorbents for pollutants removal from aqueous solutions, Innovation, 2 (2021) 100076, doi: 10.1016/j.xinn.2021.100076.
[16] S. Raghav, D. Kumar, Adsorption equilibrium, kinetics, and thermodynamic studies of fluoride adsorbed by tetrametallic oxide adsorbent, J. Chem. Eng. Data, 63 (2018) 1682–1697.
[17] S. Ghosh, D. Mitra, In: A.K. Sarma, V.P. Singh, R.K. Bhattacharjya, S.A. Kartha, Eds., Urban Ecology, Water Quality and Climate Change, Springer, Switzerland, 2018, pp. 267–274.
[18] S. Mitra, A. Sarkar, S. Sen, Removal of chromium from industrial effluents using nanotechnology: a review, Nanotechnol. Environ. Eng., 2 (2017) 1–14.
[19] X. Yang, T. Zhou, B. Ren, A. Hursthouse, Y. Zhang, Removal of Mn(II) by sodium alginate/graphene oxide composite double-network hydrogel beads from aqueous solutions, Sci. Rep., 8 (2018) 1–16.
[20] A. Abu-Nada, G. McKay, A. Abdala, Recent advances in applications of hybrid graphene materials for metals removal from wastewater, Nanomaterials, 10 (2020) 595, doi: 10.3390/nano10030595.
[21] N. Zaaba, K. Foo, U. Hashim, S. Tan, W.-W. Liu, C. Voon, Synthesis of graphene oxide using modified hummers method: solvent influence, Proc. Eng., 184 (2017) 469–477.
[22] H. Pearson, D. Mara, C. Bartone, Guidelines for the minimum evaluation of the performance of full-scale waste stabilization pond systems, Water Res., 21 (1987) 1067–1075.
[23] M.Z. Iqbal, A.A. Abdala, Thermally reduced graphene: synthesis, characterization and dye removal applications, RSC Adv., 3 (2013) 24455–24464.
[24] J. Wang, B. Chen, Adsorption and coadsorption of organic pollutants and a heavy metal by graphene oxide and reduced graphene materials, Chem. Eng. J., 281 (2015) 379–388.
[25] P. Tan, J. Sun, Y. Hu, Z. Fang, Q. Bi, Y. Chen, J. Cheng, Adsorption of Cu^{2+}, Cd^{2+} and Ni^{2+} from aqueous single metal solutions on graphene oxide membranes, J. Hazard. Mater., 297 (2015) 251–260.
[26] R.L. White, C.M. White, H. Turgut, A. Massoud, Z.R. Tian, Comparative studies on copper adsorption by graphene oxide and functionalized graphene oxide nanoparticles, J. Taiwan Inst. Chem. Eng., 85 (2018) 18–28.
[27] D.M. Mahmudunnabi, M.Z. Alam, M. Nurnabi, Removal of TURQUOISE GN from aqueous solution using graphene oxide, Desal. Water Treat., 174 (2020) 389–399.
[28] C. Valencia, C.H. Valencia, F. Zuluaga, M.E. Valencia, J.H. Mina, C.D. Grande-Tovar, Synthesis and application of scaffolds of chitosan-graphene oxide by the freeze-drying method for tissue regeneration, Molecules, 23 (2018) 2651, doi: 10.3390/molecules23102651.
[29] G. Blázquez, F. Hernáinz, M. Calero, M.A. Martín-Lara, G. Tenorio, The effect of pH on the biosorption of Cr(III) and Cr(VI) with olive stone, Chem. Eng. J., 148 (2009) 473–479.
[30] A. Bedemo, B.S. Chandravanshi, F. Zewge, Removal of trivalent chromium from aqueous solution using aluminum oxide hydroxide, Springer Plus, 5 (2016) 1–11.
[31] V.C.G.D. Santos, A.d.P.A. Salvado, D.C. Dragunski, D.N.C. Peraro, C.R.T. Tarley, J. Caetano, Highly improved chromium(III) uptake capacity in modified sugarcane bagasse using different chemical treatments, Quím. Nova, 35 (2012) 1606–1611.
[32] Y. Abshirini, R. Foroutan, H. Esmaeili, Cr(VI) removal from aqueous solution using activated carbon prepared from *Ziziphus Spina–Christi* leaf, Mater. Res. Exp., 6 (2019) 045607, doi: 10.1088/2053-1591/aafb45.
[33] Y. Qiu, Q. Zhang, B. Gao, M. Li, Z. Fan, W. Sang, H. Hao, X. Wei, Removal mechanisms of Cr(VI) and Cr(III) by biochar supported nanosized zero-valent iron: synergy of adsorption, reduction and transformation, Environ. Pollut., 265 (2020) 115018, doi: 10.1016/j.envpol.2020.115018.
[34] O. Sahu, N. Singh, In: Shahid-ul-Islam, B.S. Butola, Eds., The Impact and Prospects of Green Chemistry for Textile Technology, Elsevier, Amsterdam, 2019, pp. 367–416.
[35] H. Patel, Fixed-bed column adsorption study: a comprehensive review, Appl. Water Sci., 9 (2019) 1–17.
[36] T. Bohli, A. Ouederni, I. Villaescusa, Simultaneous adsorption behavior of heavy metals onto microporous olive stones activated carbon: analysis of metal interactions, Euro-Meditt. J. Environ. Integr., 2 (2017) 1–15.
[37] H. Vu, T. Frydl, P. Dvorak, J. Selucka, P. Starkova, In: L. Zhang, J.W. Drelich, N.R. Neelameggham, D.P. Guillen, N. Haque, J. Zhu, Z. Sun, T. Wang, J.A. Howarter, F. Tesfaye, S. Ikhmayies, E. Olivetti, M.W. Kennedy, Eds., Energy Technology, Springer, Switzerland, 2017, pp. 229–238.

[38] E. Aranda-García, E. Cristiani-Urbina, Hexavalent chromium removal and total chromium biosorption from aqueous solution by *Quercus crassipes* acorn shell in a continuous up-flow fixed-bed column: influencing parameters, kinetics, and mechanism, PLoS One, 15 (2020) e0227953, doi: 10.1371/journal.pone.0227953.
[39] P.V. Lopez-Nuñez, E. Aranda-García, M.d.C. Cristiani-Urbina, L. Morales-Barrera, E. Cristiani-Urbina, Removal of hexavalent and total chromium from aqueous solutions by plum (*P. domestica* L.) tree bark, Environ. Eng. Manage. J., 13 (2014) 1927–1938.
[40] G.P. Jeppu, T.P. Clement, A modified Langmuir–Freundlich isotherm model for simulating pH-dependent adsorption effects, J. Contam. Hydrol., 129 (2012) 46–53.
[41] M. Iqbal, A. Abdala, Thermally reduced graphene: synthesis, characterization and dye removal applications, RSC Adv., 3 (2013) 24455–24464.
[42] N.K. Mondal, S. Chakraborty, Adsorption of Cr(VI) from aqueous solution on graphene oxide (GO) prepared from graphite: equilibrium, kinetic and thermodynamic studies, Appl. Water Sci., 10 (2020) 1–10.
[43] H. Li, Z. Chi, J. Li, Covalent bonding synthesis of magnetic graphene oxide nanocomposites for Cr(III) removal, Desal. Water Treat., 52 (2014) 1937–1946.
[44] L.P. Lingamdinne, I.-S. Kim, J.-H. Ha, Y.-Y. Chang, J.R. Koduru, J.-K. Yang, Enhanced adsorption removal of Pb(II) and Cr(III) by using nickel ferrite-reduced graphene oxide nanocomposite, Metals, 7 (2017) 225, doi: 10.3390/met7060225.
[45] L.P. Lingamdinne, J.R. Koduru, Y.-L. Choi, Y.-Y. Chang, J.-K. Yang, Studies on removal of Pb(II) and Cr(III) using graphene oxide based inverse spinel nickel ferrite nanocomposite as sorbent, Hydrometallurgy, 165 (2016) 64–72.
[46] S. Yang, L. Li, Z. Pei, C. Li, J. Lv, J. Xie, B. Wen, S. Zhang, Adsorption kinetics, isotherms and thermodynamics of Cr(III) on graphene oxide, Colloids Surf., A, 457 (2014) 100–106.
[47] X. Yang, Y. Wan, Y. Zheng, F. He, Z. Yu, J. Huang, H. Wang, Y.S. Ok, Y. Jiang, B. Gao, Surface functional groups of carbon-based adsorbents and their roles in the removal of heavy metals from aqueous solutions: a critical review, Chem. Eng. J., 366 (2019) 608–621.
[48] E.C. Lima, A.A. Gomes, H.N. Tran, Comparison of the nonlinear and linear forms of the van't Hoff equation for calculation of adsorption thermodynamic parameters ($\Delta S°$ and $\Delta H°$), J. Mol. Liq., 311 (2020) 113315, doi: 10.1016/j.molliq.2020.113315.
[49] ECR, Ministry of Environment and Forest (MoEF) Government of People's Republic of Bangladesh, Environmental Conservation Rules, 1997, pp. 221–222.
[50] F. Teshale, R. Karthikeyan, O. Sahu, Synthesized bioadsorbent from fish scale for chromium(III) removal, Micron, 130 (2020) 102817, doi: 10.1016/j.micron.2019.102817.
[51] C. Bai, L. Wang, Z. Zhu, Adsorption of Cr(III) and Pb(II) by graphene oxide/alginate hydrogel membrane: characterization, adsorption kinetics, isotherm and thermodynamics studies, Int. J. Biol. Macromol., 147 (2020) 898–910.
[52] S.B. Lyubchik, I.I. Perepichka, O.L. Galushko, A.I. Lyubchik, E.S. Lygina, I.M. Fonseca, Optimization of the conditions for the Cr(III) adsorption on activated carbon, Adsorption, 11 (2005) 581–593.